Anal Bioanal Chem (2009) 394:329–336
DOI 10.1007/s00216-009-2616-0

ORIGINAL PAPER

Fast-scan cyclic voltammetry for the detection of tyramine and octopamine

Stephanie E. Cooper · B. Jill Venton

Received: 31 October 2008 / Revised: 23 December 2008 / Accepted: 9 January 2009 / Published online: 3 February 2009

Abstract Tyramine and octopamine are biogenic amine neurotransmitters in invertebrates that have functions analogous to those of the adrenergic system in vertebrates. Trace amounts of these neurotransmitters have also been identified in mammals. The purpose of this study was to develop an electrochemical method using fast-scan cyclic voltammetry at carbon-fiber microelectrodes to detect fast changes in tyramine and octopamine. Because tyramine is known to polymerize and passivate electrode surfaces, waveform parameters were optimized to prevent passivation. No fouling was observed for octopamine when the electrode was scanned from 0.1 to 1.3 V and back at 600 V/s, while a small decrease of less than 10% of the signal was seen for 15 repeated exposures to tyramine. The technique has limits of detection of 18 nM for tyramine and 30 nM for octopamine, much lower than expected levels in insects and lower than basal levels in some brain regions of mammals. Current was linear with concentration up to 5 μM. This voltammetry technique should be useful for measuring tyramine and octopamine changes in insects, such as the fruit fly, *Drosophila melanogaster*.

Keywords Phenolamine · Microelectrode · Catecholamine · Fruit fly · *Drosophila* · Polytyramine

Introduction

Tyramine and octopamine are important neurotransmitters in invertebrates, serving functions analogous to those of the vertebrate adrenergic neurotransmitters norepinephrine and epinephrine [1]. Tyramine is a decarboxylation product of tyrosine and the biological precursor of octopamine. In invertebrates, octopamine plays a role in initiation of behaviors and stress responses as well as regulation of sensory systems, including pheromone response, taste, vision, and olfaction [2, 3]. Less is known about the function of tyramine, although it has been implicated in olfaction, muscle contraction, and cocaine sensitization [4]. Receptors for both compounds have been identified in insects [5, 6], and it has been suggested that interrupting tyramine or octopamine signaling might be a valuable strategy for insecticides, because they would show negligible vertebrate toxicity. While trace concentrations of octopamine and tyramine have been isolated in vertebrate brain tissue, the concentrations are 100 times lower than in invertebrates [7]. Initially, they were thought to be just metabolic by-products, but the discovery of a family of receptors that are activated by tyramine and octopamine in mammals has led to renewed interest as these trace amines may be functional [8]. In particular, some of the highest concentrations of the trace amines are found in the caudate putamen [9, 10], where they may be involved in potentiating the response of dopamine.

Jill Venton is an Assistant Professor of Chemistry and Neuroscience at the University of Virginia. She has received an NSF CAREER award and the Eli Lilly Young Analytical Investigator Award. Her research interests include developing new microelectrodes and in vivo detection of neurotransmitters.

S. E. Cooper · B. J. Venton (✉)
Department of Chemistry, University of Virginia,
P.O. Box 400319, Charlottesville, VA 22904-4319, USA
e-mail: jventon@virginia.edu

The most common methods for studying the tyramine and octopamine systems are immunohistochemistry methods that can identify populations of neurons [1, 11], but they are not effective for quantitation of neurotransmitter concentrations. More recently, separation techniques have been developed for quantitative analysis. A high performance liquid chromatography method with electrochemical detection has been used to separate and detect picogram levels of the biogenic amines dopamine, serotonin, octopamine, and tyramine [12]. However, the amperometric detection scheme with high oxidation potentials necessary for octopamine and tyramine leads to electrode instability and degradation. A capillary electrophoresis–electrochemical detection method has also been developed that can measure amine levels in single fly brains. Fourteen amines, including octopamine and tyramine, can be separated and quantitated in 20 min [13]. These techniques are useful in determining basal levels of biogenic amines and how basal levels change after genetic mutations. However, all these separation methods require that the insect brains be homogenized, so they are not useful for making repeated measurements in one sample.

Tyramine and octopamine are structurally similar to other biogenic amine neurotransmitters but are phenolamines instead of catecholamines. The electrochemistry of tyramine has been studied at a variety of electrodes [14–17]. Like other phenols, the oxidation of tyramine produces a phenoxy radical, which can subsequently react with another tyramine molecule to form a *para*-linked dimer. Further oxidation leads to polymerization that can result in the formation of a passivating, insulating layer on the electrode [14]. Therefore, one challenge in developing an electrochemical method for tyramine and octopamine detection is to avoid fouling of the electrode by polymerized products. Few studies have characterized octopamine electrochemistry, but it is likely to be similar to that of tyramine. Tyramine and octopamine have a rapid turnover rates in vivo [18], similar to other monoamines, so concentrations are expected to change rapidly. Therefore, rapid measurements with fast electrochemical techniques such as fast-scan cyclic voltammetry at microelectrodes would be ideal for making fast, repeated measurements of octopamine and tyramine with minimal tissue damage [19]. Carbon-fiber microelectrodes are less than 7 μm in diameter, so they are small enough to be inserted into fruit fly brains [20, 21] or the brains of other insects. However, the electrochemistry of tyramine and octopamine has not been characterized at carbon-fiber microelectrodes.

The goal of the work reported here was to develop a fast scan cyclic voltammetry method to detect octopamine and tyramine. The electrochemistry of each compound was studied and an optimized waveform was developed to minimize fouling associated with side products. The detection of octopamine and tyramine was linear up to 5 μM and limits of detection of less than 30 nM would be sufficient to detect concentration changes in invertebrate samples, such as the fruit fly.

Experimental

Solutions

The experiments were carried out in a buffer appropriate for invertebrate experiments. The salt concentrations in the buffer were adapted from Schneider's insect medium, which is used to stably culture insect nerve cords and neurons [22]. The buffer concentrations were 15.2 mM $MgSO_4 \cdot 7H_2O$, 21 mM KCl, 3.3 mM KH_2PO_4, 36 mM NaCl, 5.8 mM NaH_2PO_4, and 5.4 mM $CaCl_2$. The buffer pH was adjusted to 6.2. For studies of the effect of pH, a simple phosphate buffer was used (3.3 mM KH_2PO_4, 5.8 mM NaH_2PO_4) and the pH was adjusted to 3.2, 6.2, or 9.2. Octopamine hydrochloride and tyramine hydrochloride were purchased from Sigma (St. Louis, MO, USA) and made up as stock solutions in 0.1 M perchloric acid. These stock solutions were diluted with the buffer to the specified concentration on the day of each experiment. All solutions were prepared using Milli-Q water (Millipore, Billerica, MA USA).

Electrodes and electrochemistry

Cylindrical carbon-fiber microelectrodes were made as previously described [23]. T-650 fibers were aspirated into glass capillaries, the capillaries pulled, and then the fibers trimmed to about 50 μm. Electrodes were epoxied to ensure a good seal (Epon resin 828, Miller-Stephenson, Danbury, CT, USA). All electrodes were soaked for 10 min in 2-propanol before use. The reference electrode was a Ag/AgCl wire.

Electrochemical data were collected using either a GeneClamp potentiostat (with a custom-modified headstage, Molecular Devices, Sunnyvale, CA, USA) or a ChemClamp potentiostat (custom-modified, Dagan, Minneapolis, MN, USA). Data were collected with a homebuilt data analysis system. TarHeel CV software was used to apply the waveform and collect and analyze the data [24].

Electrodes were tested using flow-injection analysis [25]. The carbon-fiber electrode was positioned at the output of a flow-injection apparatus. A six-port high performance liquid chromatography loop injector was mounted on an air actuator (Valco, Houston, TX, USA) that received digital signals from the software to turn the valve and allow the sample to flow by the electrode. Four-second injections of the compound of interest were used to mimic fast concentration changes expected in biological systems. All results were background-subtracted using an average of ten

background cyclic voltammograms from the preinjection time. For current versus time traces, the current was integrated in a 100-mV window centered around the oxidation peak.

Statistics

All averages are given as the mean ± standard error of the mean for *n* electrodes. Error bars in graphs are also given as the standard error of the mean. Statistics were calculated using GraphPad Prism (GraphPad Software, La Jolla, CA, USA).

Results and discussion

The structures of tyramine and octopamine are similar to those of dopamine and norepinephrine, respectively, except that they are phenolamines. Therefore, they have just one hydroxyl group on the phenyl ring instead of the two in the catecholamines (Fig. 1). The most common geometry in vivo is the *para* isomer, although *meta* isomers have been isolated in mammals at very low concentrations [7].

Characterization of octopamine and tyramine electrochemistry using fast-scan cyclic voltammetry

For catecholamine detection with carbon-fiber microelectrodes, the electrode is typically ramped from -0.4 to 1.0 V and back at around 400 V/s. The oxidation potentials of octopamine and tyramine were expected to be higher than that for dopamine [12, 14], so a waveform from -0.4 to 1.3 V and back at 400 V/s was initially used, with a repetition rate of 10 Hz. Fast scanning with cyclic voltammetry produces large background currents that are temporally stable and can be subtracted out [25]. Figure 1

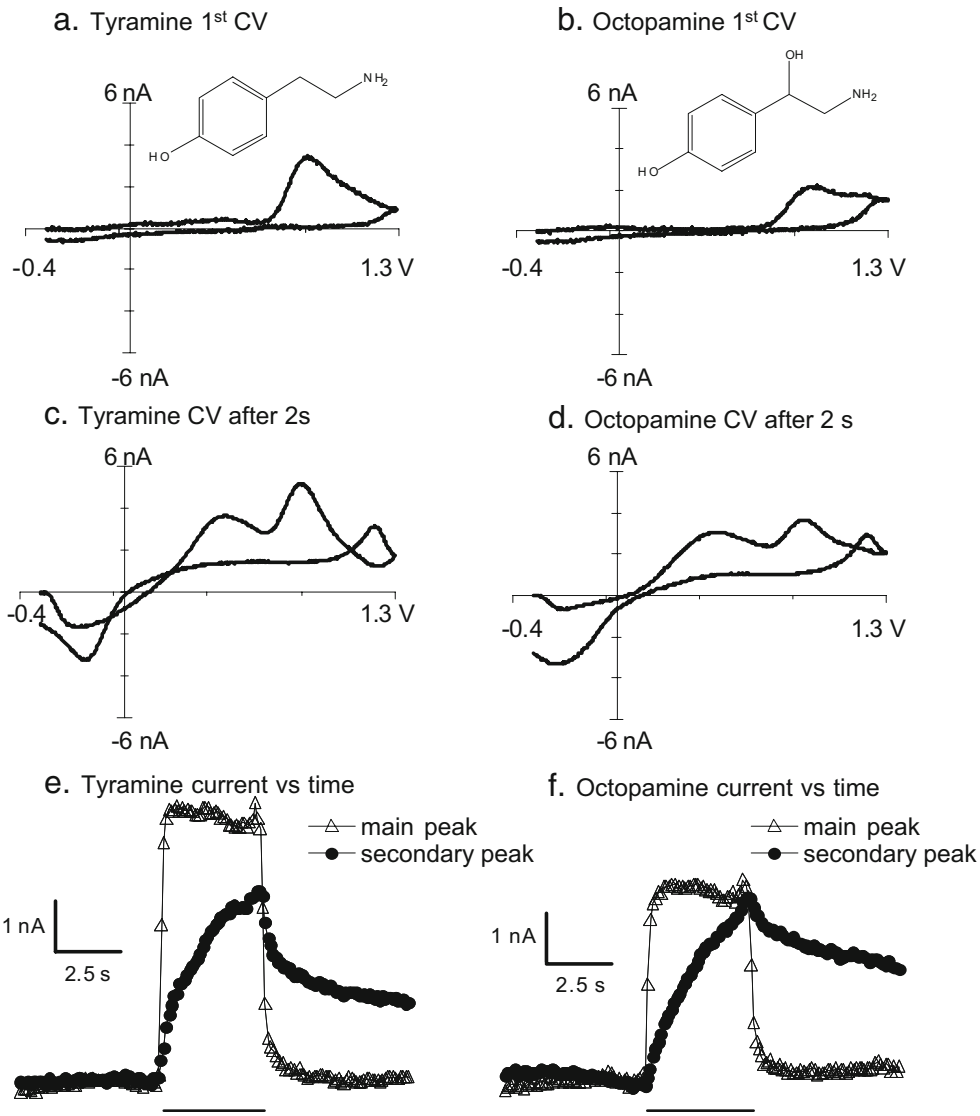

Fig. 1 Electrochemical characterization of 1 μM tyramine and 1 μM octopamine using normal cyclic voltammetry parameters. The electrode was scanned from -0.4 to 1.3 V and back at 400 V/s every 100 ms. *Top*: The first background-subtracted cyclic voltammogram (*CV*) after exposure to **a** tyramine or **b** octopamine. The main oxidation peak is at 0.85 V for tyramine and 0.9 V for octopamine. The structure of each molecule is shown as an *inset*. *Middle*: CVs after 2 s of exposure to **c** tyramine or **d** octopamine. These plots show the presence of both the main oxidation peak that was observed in the first CV as well as a secondary oxidation peak around 0.5 V and a reduction peak around -0.2 V. *Bottom*: The current versus time traces show the electrode response for the main peak (*triangles*) and the secondary peak (*circles*) for **e** tyramine and **f** octopamine. The *bar* indicates when the electrode was exposed to the compound. Note the square response of the main peak to the injection, but the slow rise and decay of the secondary peak

shows background-subtracted cyclic voltammograms and current versus time traces at the oxidation potentials. The mechanism of the oxidation steps is revealed by the cyclic voltammograms. The first cyclic voltammogram collected has a main oxidation peak at 0.85 V for tyramine and at 0.9 V for octopamine. No reduction peak was detected, indicating either that the reaction was not reversible or that the oxidation product quickly underwent a reaction to another material. Figure 1 also shows cyclic voltammograms collected 2 s after initial exposure to the compound, the 20th cyclic voltammograms collected. These cyclic voltammograms have additional peaks due to a secondary product that forms. The secondary oxidation peak occurs around 0.5 V and a corresponding reduction peak is also detected at -0.2 V. Also, a small oxidative current is seen at the switching potential.

The bottom traces show the changes in current at the oxidation peaks over time. The main peak, around 0.9 V, has a square response to the injection of a square pulse of analyte. However, the secondary peak, around 0.5 V, has a very different profile, as it takes longer to reach its peak current and does not return to the baseline, even after tyramine or octopamine have been washed out of the flow cell. The continued presence of this oxidation peak after tyramine or octopamine has been removed suggests that it results from a product that is adsorbed to the electrode. The slow rise indicates that this product is formed after the initial oxidation, likely from a side reaction formed from the initial oxidized species.

The current versus time traces in Fig. 1 are on the same scale and they indicate that the electrodes are more sensitive for tyramine detection than for octopamine detection. On average, a current of 6.0±0.9 nA is detected for the main oxidation peak of 1 μM tyramine, which is significantly different from the 4.2±0.7 nA detected for the same concentration of octopamine (p=0.0016 paired t test, n=8 electrodes). The voltages corresponding to the locations of the main oxidation peaks are also slightly different. The average peak oxidation voltage for tyramine was 0.89± 0.02, while it was 0.94±0.02 for octopamine (p=0.0017, paired t test, n=8 electrodes). However, there would not be enough resolution to tell them apart in a mixture. In this way, they are similar to dopamine and norepinephrine, which are also indistinguishable with fast-scan cyclic voltammetry [26].

Mechanism of tyramine and octopamine oxidation

Tyramine, like many phenols, is known to polymerize after oxidation [15, 27]. Polytyramine has been shown to passivate electroactive surfaces and has been used as a substrate for immobilizing enzymes in enzyme-modified electrodes [28]. The polymer is formed by electrodeposition with cyclic voltammetry, using scanning limits very similar to those used for our initial detection scheme [28]. Therefore, we believe that tyramine and octopamine are polymerizing and being deposited on the electrode. A previous electrochemical study using slow-scan cyclic voltammetry showed oxidation peaks at both 1.0 and 0.4 V for tyramine [14], similar to our studies. A reduction peak was also detected in that study that corresponds to the secondary oxidation peak. These peaks at the lower potential were not present on the first scan and are attributed to the covering of the surface by the electroactive polytyramine film. Polymer attaching to the electrode would passivate the surface, which means the electrode would not be amenable to long-term detection of tyramine and octopamine. Indeed, the current measured for tyramine decreased by an average of 12±1% for just three repeated injections for a flow injection analysis experiment (n=8).

To gain insight into the possible mechanism of tyramine and octopamine detection, we examined the effect of pH on tyramine and octopamine oxidation. Figure 2 shows that the main oxidation potential for tyramine and octopamine shifts to less positive potentials with increasing pH.

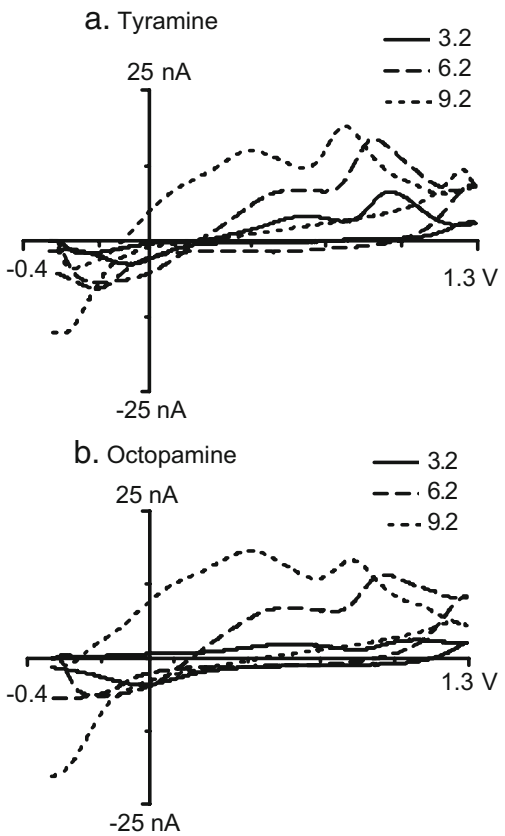

Fig. 2 Effect of pH: **a** 1 μM tyramine and **b** 1 μM octopamine electrochemistry in pH 3.2 (*solid line*), 6.2 (*dashed line*), or 9.2 (*dotted line*) phosphate buffer. The electrode was scanned from -0.4 to 1.3 V and back at 400 V/s every 100 ms

Scheme 1 Oxidation mechanism for tyramine (R is H) and octopamine (R is OH)

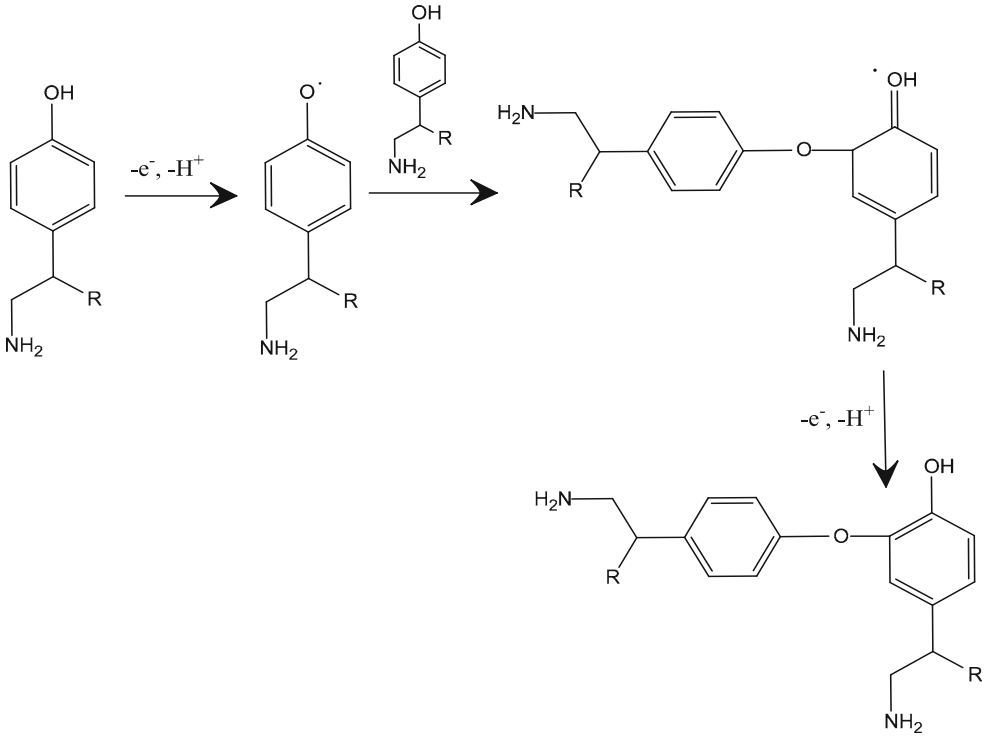

Scheme 1 shows the likely mechanism for oxidation. The first step is one-electron oxidation of the phenol species. The easier oxidation in a more basic solution is consistent with previous observations that the phenolate anion is more easily oxidized than the phenol [14]. The secondary peak is also larger at greater pH values, which is consistent with the polymerization mechanism in Scheme 1 that generates H^+ions [15]. After the initial oxidation, the radical can react with another phenol to form a radical dimer, which can undergo another one-electron oxidation. This product can continue to react with other phenols to form a polymer.

Effect of different scanning parameters

To minimize the effects of polymerized side products and passivation of the electrode, we explored the effects of using different cyclic voltammetry waveforms. First, we tested the effect of using different switching potentials (Fig. 3a, b) while keeping the holding potential at -0.4 V and the scan rate at 400 V/s. Increasing the switching potential increases the current detected for the main oxidation peak for tyramine and octopamine, except that there is little difference for 1.4 and 1.5 V. However, as the switching potential increased, the amount of side product detected also increased substantially, particularly for octopamine. At the highest switching potentials, the secondary product peak for octopamine was larger than the main peak (Fig. 3b). With lower switching potentials, the amplitude of the secondary product peaks was less, but the main oxidation peak was also lower and the peak occurred so close to the switching potential that it was not well defined on the cyclic voltammogram.

From that study, we picked a switching potential of 1.3 V as a middle ground between main oxidation peak sensitivity and side product peak formation. With 1.3 V, the oxidation peak is clearly visible on the cyclic voltammogram. The effect of holding potential was then tested (Fig. 3c, d). The largest sensitivity was found with the most negative switching potentials. This is not surprising, as the amine groups are expected to be protonated on tyramine and octopamine, making them cations at pH 6.2. Therefore, they would adsorb to a negatively charged electrode, similar to catecholamines [29]. The main oxidation peaks for tyramine and octopamine could be detected using positive holding potentials as well. The secondary product amplitude also decreased with increased holding potential and side products were not detected with positive holding potentials. While the dimerization reaction would still be expected to occur in solution, the products are likely not adsorbing to the electrode. To minimize fouling by side products, a holding potential of 0.1 V was chosen for further studies.

One way to increase the current detected with cyclic voltammetry is to increase the scan rate. A plot of example cyclic voltammograms from one electrode, scanned from 0.1 to 1.3 V and back for scan rates ranging from 200 to 1,000 V/s, is shown in Fig. 4. The current for the main oxidation peak did increase with scan rate, as expected. The oxidation peak around 1.2 V increased with scan rate as well, and is most visible for octopamine. This peak was observed with the -0.4 to 1.3 V waveform (Fig. 1) but

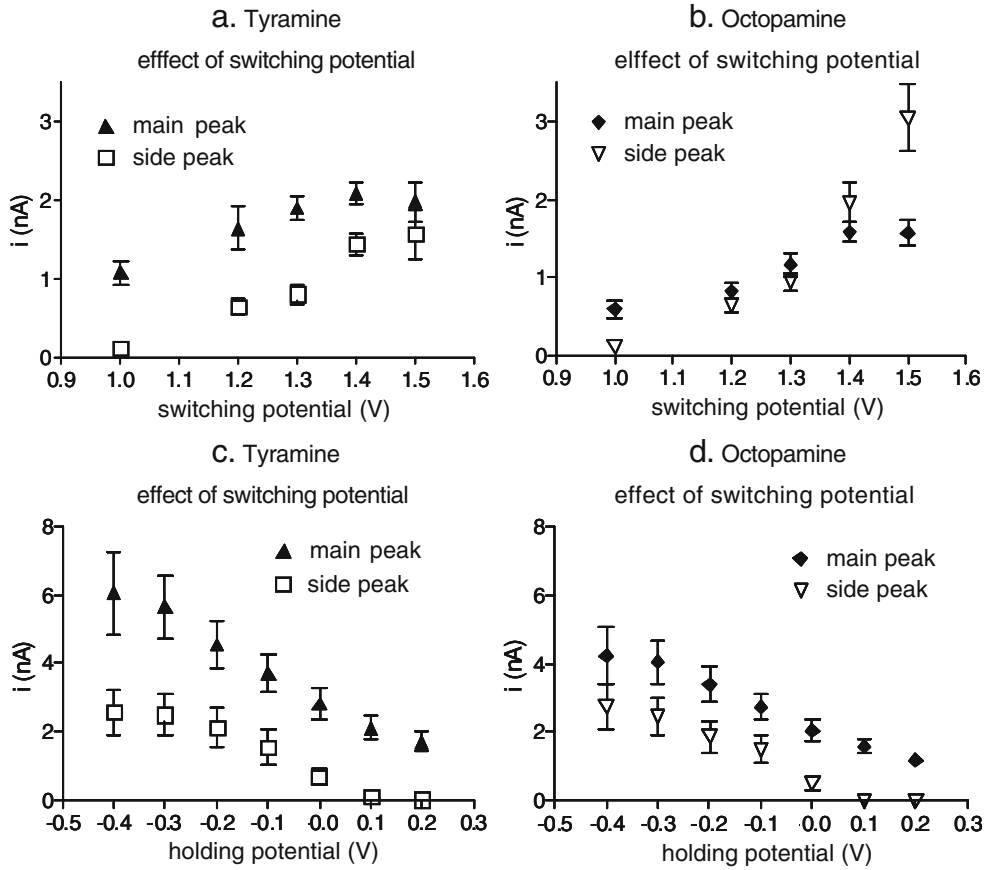

Fig. 3 Effect of holding potential and switching potential on oxidation peak currents. To test the effect of switching potential, the holding potential was held constant at -0.4 V, the scan rate at 400 V/s, and the switching potential varied between 1.0 and 1.5 V. *Error bars* are the standard error of the mean (SEM) (n=4 electrodes). **a** For 1 μM tyramine, the main oxidation peak (*triangles*) is always larger than the side product peak (*squares*), but the side product peak is greater at larger switching potential values. **b** For 1 μM octopamine, the side product peak (*triangles*) increases at a greater rate with increased switching potential than the main peak (*diamonds*). To test the effect of holding potential, the switching potential was held constant at 1.3 V, the scan rate at 400 V/s, and the holding potential varied from -0.4 to 0.2 V. **c** For 1 μM tyramine, both the side product peak and the main peak decrease with increasing holding potential, with no side product peak detected at positive potentials. **d** For 1 μM octopamine, the trends are similar to those for tyramine with decreasing signals at positive holding potentials

appears more prominent with the 0.1–1.3-V waveform because polytyramine is not being deposited on the electrode and peaks associated with the polymer are not being detected. This latter peak may represent oxidation of the amine to an imine or another product that forms after initial tyramine oxidation. Because of this extra peak, an optimum scan rate of 600 V/s was chosen. To test whether the kinetics are adsorption- or diffusion-controlled, a plot of current versus the square root of scan rate was made with scan rates from 20 to 1,000 V/s. The plot was linear, with an average R^2 value for four electrodes of 0.993 for tyramine and 0.992 for octopamine, indicating the kinetics are diffusion-controlled.

Characterization of the optimized waveform

An optimized waveform from 0.1 to 1.3 V and back at 600 V/s, every 100 ms, was chosen and then characterized. Figure 5 shows cyclic voltammograms and current versus time traces for the optimized waveform. The cyclic voltammograms, taken 2 s after the initial exposure to the compound, show the presence of a main oxidation peak around 0.9 V, and also a peak near the switching potential. However, the secondary product peak at 0.5 V is not present (cf. Fig. 1). Because the potentials scanned are still sufficient for the secondary peak to be produced, the absence of the side product peak points to less adsorption of the secondary oxidation products on the electrode with the positive holding potential.

The current versus time traces for the main oxidation peak show a very square response to the square plug of analyte. No products continue to be oxidized after tyramine or octopamine has been washed out of the flow cell, indicating that the oxidation products are not adsorbing to the electrode. The sensitivity for tyramine is higher than that for octopamine, with an average current of 3.2±0.3

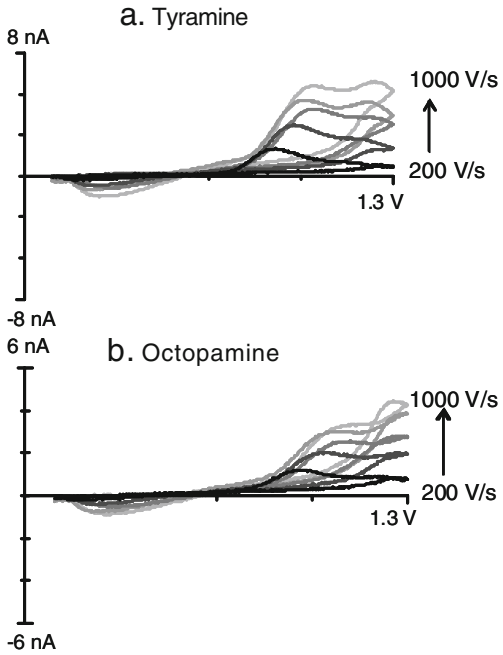

Fig. 4 Effect of scan rate on the observed potential for **a** 1 μM tyramine and **b** 1 μM octopamine. The electrode was scanned from 0.1 to 1.3 V and back at scan rates of 200, 400, 600, 800, and 1,000 V/s. The main oxidation peak around 0.85 V increases with scan rate and a secondary oxidation peak at 1.2 V becomes more apparent with increasing scan rate

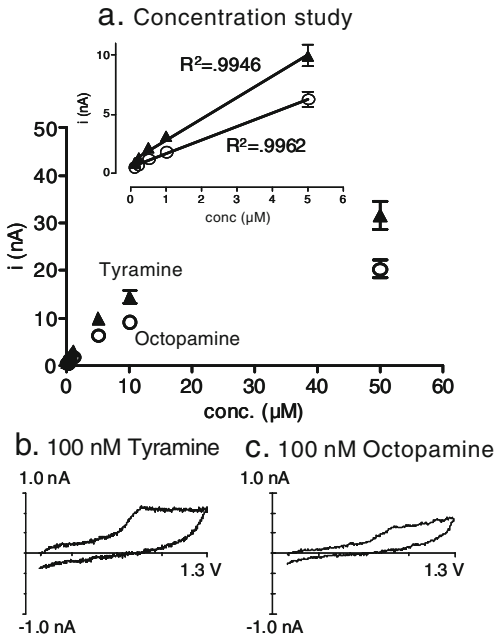

Fig. 6 Concentration study using the optimized waveform. **a** The concentration of octopamine (*circles*) and tyramine (*triangles*) was varied from 0.2 to 50 μM. The *inset* shows that the current for the main oxidation peak was linear with concentration up to 5 μM for each compound. *Error bars* are SEM, $n=5$. CVs for **b** 100 nM tyramine and **c** 100 nM octopamine

nA for 1 μM tyramine compared with 1.9±0.2 nA for octopamine ($p=0.0016$, $n=9$ electrodes).

To test for the possibility of fouling, 15 consecutive flow-injection experiments were run, where the electrode was exposed to a 4-s bolus of analyte every 20 s. For octopamine, there is no evidence of fouling as the signal for the 15th injection is the same as the signal for the first injection (100±2%). For tyramine, a slight amount of

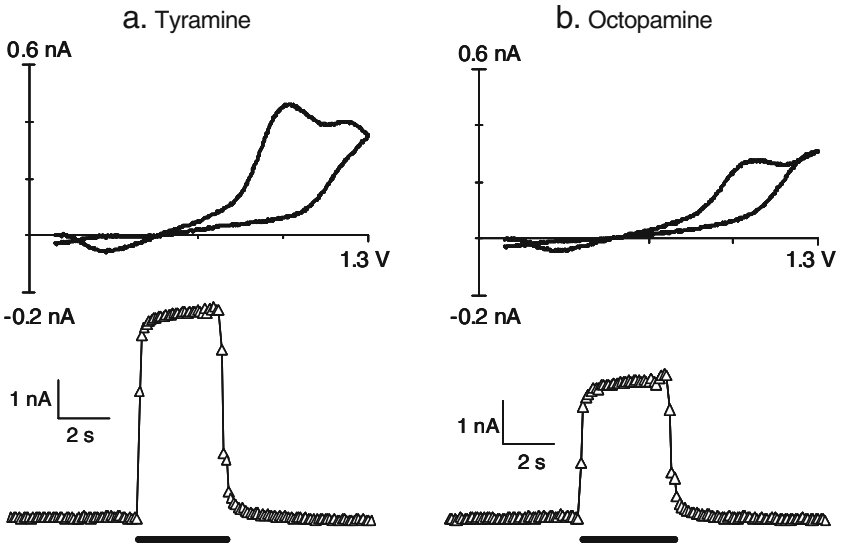

Fig. 5 Detection using the optimized waveform. The electrode was scanned from 0.1 to 1.3 V and back at 600 V/s at 10 Hz. **a** For 1 μM tyramine, the CV reveals a main oxidation peak at 0.96 V and another near the switching potential, but no side product peak around 0.5 V. The current versus time response for the main peak is square. The *bar* indicates the exposure time to the analyte. **b** For 1 μM octopamine, the main oxidation peak is at 1.01 V. The oxidation peak at the switching potential is of about the same magnitude as the main peak and is also evident in the CV. The current versus time plot indicates a square response to the bolus of octopamine

fouling is observed, but the signal after the 15th injection is still 90±1% of the original signal (n=4). The last five injections have similar currents, showing that the fouling may plateau. This indicates that some minimal passivation is still occurring with this waveform, but the amount of fouling with the positive holding potential waveform is substantially less than when the electrode is scanned from -0.4 V (Fig. 1).

The response of electrodes to a range of concentrations was tested to determine the linear range of the electrode for octopamine and tyramine detection (Fig. 6). The peak oxidation currents were linear up to 5 μM for octopamine and tyramine. Cyclic voltammograms for the lowest concentrations, 100 nM, illustrate that low concentrations can be detected. Limits of detection were estimated on the basis of the average signal-to-noise values from the 100 nM concentration. Therefore, if we could detect a signal 3 times the noise, the limit of detection would be 18 nM for tyramine and 30 nM for octopamine. These concentrations are smaller than concentrations found in invertebrates [12], where neurotransmitter concentration changes would be on the order of hundreds of nanomoles per liter to micromoles per liter levels. Therefore, the sensitivity should be sufficient for invertebrate use. For vertebrates, the tissue content levels are lower, in the tens to hundreds of nanomoles per liter range, but the electrodes might still be sensitive enough to detect the trace amines in some regions [7].

Conclusions and future directions

We have developed a method for detection of octopamine and tyramine using carbon-fiber microelectrodes that will allow measurements of fast concentration changes. Optimizing the fast scan cyclic voltammetry waveform gives a method where there is minimal fouling of the electrode by polymerized oxidation products. Octopamine and tyramine have similar electrochemical signatures, as they differ by only one hydroxyl group. Therefore, similar to other compounds such as dopamine and norepinephrine, they cannot be distinguished solely by electrochemistry. To detect these molecules in a real sample, a pharmacological strategy would need to be employed. For example, octopamine is synthesized from tyramine in the invertebrate by tyrosine-β-hydroxylase, so an inhibitor of this enzyme would eliminate octopamine changes and allow only tyramine concentration changes to be measured. Alternatively, one could detect an exogenously applied neurotransmitter, so the identity of the analyte is known, and study the diffusion and clearance mechanisms. Because of the small size of carbon-fiber microelectrodes, this method should be amenable for use in small invertebrate nerve tissue samples.

Acknowledgement This work was support by a grant from the National Science Foundation (CHE 0645587).

References

1. Roeder T (2005) Annu Rev Entomol 50:447–477
2. Roeder T (1999) Prog Neurobiol 59:533–561
3. Wragg RT, Hapiak V, Miller SB, Harris GP, Gray J, Komuniecki PR, Komuniecki RW (2007) J Neurosci 27:13402–13412
4. McClung C Hirsh J (1999) Curr Biol 9:853–860
5. Cazzamali G, Klaerke DA, Grimmelikhuijzen CJ (2005) Biochem Biophys Res Commun 338:1189–1196
6. Evans PD, Maqueira B (2005) Invert Neurosci 5:111–118
7. Berry MD (2004) J Neurochem 90:257–271
8. Borowsky B, Adham N, Jones KA, Raddatz R, Artymyshyn R, Ogozalek KL, Durkin MM, Lakhlani PP, Bonini JA, Pathirana S, Boyle N, Pu X, Kouranova E, Lichtblau H, Ochoa FY, Branchek TA, Gerald C (2001) Proc Natl Acad Sci USA 98:8966–8971
9. Molinoff PB, Axelrod J (1972) J Neurochem 19:157–163
10. Boulton AA (1976) Adv Biochem Psychopharmacol 15:57–67
11. Monastirioti M, Gorczyca M, Rapus J, Eckert M, White K, Budnik V (1995) J Comp Neurol 356:275–287
12. Hardie SL, Hirsh J (2006) J Neurosci Methods 153:243–249
13. Paxon TL, Powell PR, Lee HG, Han KA, Ewing AG (2005) Anal Chem 77:5349–5355
14. de Castro CM, Vieira SN, Goncalves RA, Brito-Madurro AG, Madurro JM (2008) J Mater Sci 43:475–482
15. Tenreiro AM, Nabais C, Correia JP, Fernandes FMSS, Romero JR, Abrantes LM (2007) J Solid State Electrochem 11:1059–1069
16. Pham MC, Lacaze PC, Dubois JE (1984) J Electrochem Soc 131:777–784
17. Luczak T (2008) J App Electrochem 38:43–50
18. Durden DA, Philips SR (1980) J Neurochem 34:1725–1732
19. Venton BJ, Wightman RM (2003) Anal Chem 75:414A–421A
20. Borue X, Venton BJ (2008) In: Abstracts of monitoring molecules in neuroscience. 12th international conference on in vivo methods, University of British Columbia, Vancouver, 10–14 Aug 2008, pp 427–429
21. Makos M, Kuklinski N.M, Han KA, Ewing AG (2008) In: Abstracts of monitoring molecules in neuroscience. 12th international conference on in vivo methods, University of British Columbia, Vancouver, 10–14 Aug 2008, p 439
22. Sykes PA, Condron BG (2005) Dev Biol 286:207–216
23. Swamy BEK, Venton BJ (2007) Anal Chem 79:744–750
24. Heien ML, Johnson MA, Wightman RM (2004) Anal Chem 76:5697–5704
25. Strand AM, Venton BJ (2008) Anal Chem 80:3708–3715
26. Baur JE, Kristensen EW, May LJ, Wiedemann DJ, Wightman RM (1988) Anal Chem 60:1268–1272
27. Dubois JE, Lacaze PC, Pham MC (1981) J Electroanal Chem 117:233–241
28. Situmorang M, Gooding JJ, Hibbert DB, Barnett D (1998) Biosens Bioelectron 13:953–962
29. Bath BD, Michael DJ, Trafton BJ, Joseph JD, Runnels PL, Wightman RM (2000) Anal Chem 72:5994–6002